Journal of Nuclear Materials 390–391 (2009) 1078–1080

Contents lists available at ScienceDirect

Journal of Nuclear Materials

journal homepage: www.elsevier.com/locate/jnucmat

Interpretation of spatially resolved helium line ratios on MAST

S. Lisgo [a,*], P. Börner [b], G.F. Counsell [c], J. Dowling [a], A. Kirk [a], R. Scannell [a], M. O'Mullane [d], D. Reiter [b], MAST Team

[a] EURATOM/UKAEA Fusion Association, D3/2.15, Culham Science Centre, Abingdon, Oxfordshire, OX14 3DB, UK
[b] Institut für Plasmaphysik, FZJ, EURATOM Association, D-52425 Jülich, Germany
[c] F4E, Josep Pla, 2, Torres Diagonal Litoral B3, 08019 Barcelona, Spain
[d] 43 Department of Physics, University of Strathclyde, Glasgow G4 0NG, UK

ARTICLE INFO

PACS:
52.55
52.20.H
52.65

ABSTRACT

The tokamak boundary plasma is inherently 2D/3D, which impedes the detailed validation of transport models due to the limited spatial coverage of most diagnostics. A potential method for determining the 2D profiles of n_e and T_e in the plasma volume is to resolve spatially the emission ratios of atomic helium, principally the lines at 667, 706 and 728 nm. Unfortunately, there are several challenges associated with this approach: the traditional use of line-of-sight spectrometer data; crowding by other impurity lines; low signal levels; reliance on accurate atomic physics; and He I meta-stables. Several of these issues are explored in the present study, which utilises tomographic reconstruction of filtered CCD camera images to measure He emission throughout the divertor. Plasma gradients are resolved and compared with results from the OSM–EIRENE code. The near-target n_e and T_e values agree with Langmuir probe measurements to within a factor ~2.

Crown Copyright © 2009 Published by Elsevier B.V. All rights reserved.

1. Introduction

The tokamak boundary plasma is inherently 2D/3D and the limited spatial coverage of most diagnostics hinders the detailed validation of plasma transport models. Ratios of line emission from atomic helium are a function of the local electron density, n_e, and temperature, T_e, and have been used to diagnose a number of plasma devices [1–5]; see [4] for a comprehensive list of references. The advance presented here is to measure the helium emission using a filtered 2D CCD camera, with the images tomographically reconstructed (assuming toroidal symmetry) to produce 2D emission profiles in the poloidal plane. This spatially resolved data (~5 mm resolution) provides direct information on the plasma structure, unlike line-of-sight integrated spectrometer measurements. Results are presented for the upper divertor region of a MAST Ohmic discharge. Interpretive modeling of the background hydrogenic plasma with OSM–EIRENE is presented for comparison with the n_e and T_e values extracted from the line ratio analysis.

2. Experiment

MAST is a low aspect ratio (A = 1.4) spherical tokamak (ST) with a maximum plasma current of 1.5 MA and (presently) up to 5 MW of neutral beam power. Resistive heating of the central solenoid limits purely inductive current drive to <1 s. MAST usually operates in a near double-null (DN) configuration, which will be essential for long-pulse spherical tokamak operation due to the small area available for power deposition on the inboard side. The current flat-top parameters for the Ohmic discharge being studied (pulse 18843) are I_p = 0.73 MA, $\bar{n}_e = 3.5 \times 10^{19}$ m^{-3}, f_{GW} = 0.5, T_0 = 700 eV, and B_0 = 0.42 T. The divertor camera images were acquired 259 ms, just before the onset of sawteeth, which significantly perturb the plasma boundary in MAST. The camera system employs a beam-splitter and two Imperx IPX-1M48-L 1 mega-pixel programmable cameras. The discharge was repeated in order to acquire data for He^{+0} (447, 588, 668, 707 and 728 nm), He^{+1} (468 nm), D_α (656 nm), C^{+1} (514 nm) and C^{+2} (465 nm). The filter bandwidths range from 1.5 to 3 nm and integration times were from 0.5 to 4 ms. He puffing was required to increase the emission level for the weak lines (447 and 728 nm), bringing the plasma content to ~10% (based on He^{+1} data and Thomson scattering data at the outer midplane).

3. Interpretive modeling of the background plasma

The OSM–EIRENE interpretive code package is used to reconstruct the plasma boundary, to provide a reference for evaluating the n_e and T_e profiles from the helium line ratio analysis. OSM is a plasma fluid code [6] and EIRENE a kinetic transport code [7] for following neutral particles. Target Langmuir probe (j_{sat}, T_e) and upstream edge Thomson scattering (n_e, T_e) radial profiles are taken as input, and the wall pumping rate is set by comparison

* Corresponding author. Tel.: +011 44 1235 466824; fax: +011 44 1235 466379.
E-mail address: steve.lisgo@ukaea.org.uk (S. Lisgo).

0022-3115/$ - see front matter Crown Copyright © 2009 Published by Elsevier B.V. All rights reserved.
doi:10.1016/j.jnucmat.2009.01.292

with high resolution linear camera D_α measurements at the midplane. Note that fits to the j_{sat}, n_e and T_e data are imposed on the plasma solution, guaranteeing a high level of agreement. Transport models are used to calculate the n_e and T_e evolution along magnetic field lines in the boundary. $T_i = T_e$ is assumed.

Comparison with divertor camera D_α data, which does not provide numerical input to the simulation, is used to benchmark the calculations. Fig. 1(a) shows the camera view of the upper divertor and 1b is the calibrated image. For a quantitative comparison with the model, pixel-based tomographic inversion [8] is used to reconstruct the D_α emission profile in the poloidal plane. The algorithm is represented by $Ax = b$, where x is the poloidal emission profile and b is the camera data. A is the 'geometry matrix', which maps the line-of-sight camera view onto a poloidal mesh and is calculated using a ray tracing code. The matrix equation is solved using damped conjugate gradient minimization [9]. The reconstruction is presented in Fig. 1(c) and the D_α profile from EIRENE in Fig. 1d. For a detailed comparison, a cross-field profile is interpolated along the dashed line indicated on the figure. The data are plotted Fig. 2(a) and shows agreement within the experimental uncertainty (~30%). By generating a series of such profiles between the outer strike-point and the x-point, and assuming that the peak value represents emission at the separatrix (which is true in the OSM–EIRENE model), profiles of D_α along the separatrix are produced; see Fig. 2(b). The discrepancy near the target is attributed to the toroidal asymmetry present in the image, in violation of the assumption made during the reconstruction.

4. Helium line ratio analysis

The He^{+0} images are processed in the same fashion as the D_α data in Fig. 1, resulting in line ratio profiles along the outer divertor separatrix leg, as in Fig. 2(b). Pairs of line ratios are then used to solve for n_e and T_e at each point along the profile using atomic data from ADAS [10] for helium line emissions (adf15_pju08 designation), e.g., the intersection between 668:728 and 728:706 contours in 'atomic data space' give a unique value of n_e and T_e for each location along the separatrix leg. Combinations of line ratios that produce reasonable profiles are plotted in Fig. 3 (many do not due to degeneracies or weak dependencies in the data), along with the OSM–EIRENE results for a pure conduction heat transport model (dashed lines).

5. Discussion and future work

The general factor ~2 agreement between the model and line ratio data is encouraging given the preliminary nature of the analysis. Notable however is the very poor match to the 668/728, 728/707 profile for T_e (black line), with these three lines generally considered to be optimal for helium studies. The divergence near the targets is also rather dramatic and may be due to broadband carbon emissions, and/or contributions to the He lines from processes other than electron impact excitation (recombination and charge-exchange). If the atomic physics models and the measured data were free from errors then all of the lines in Fig. 3 would

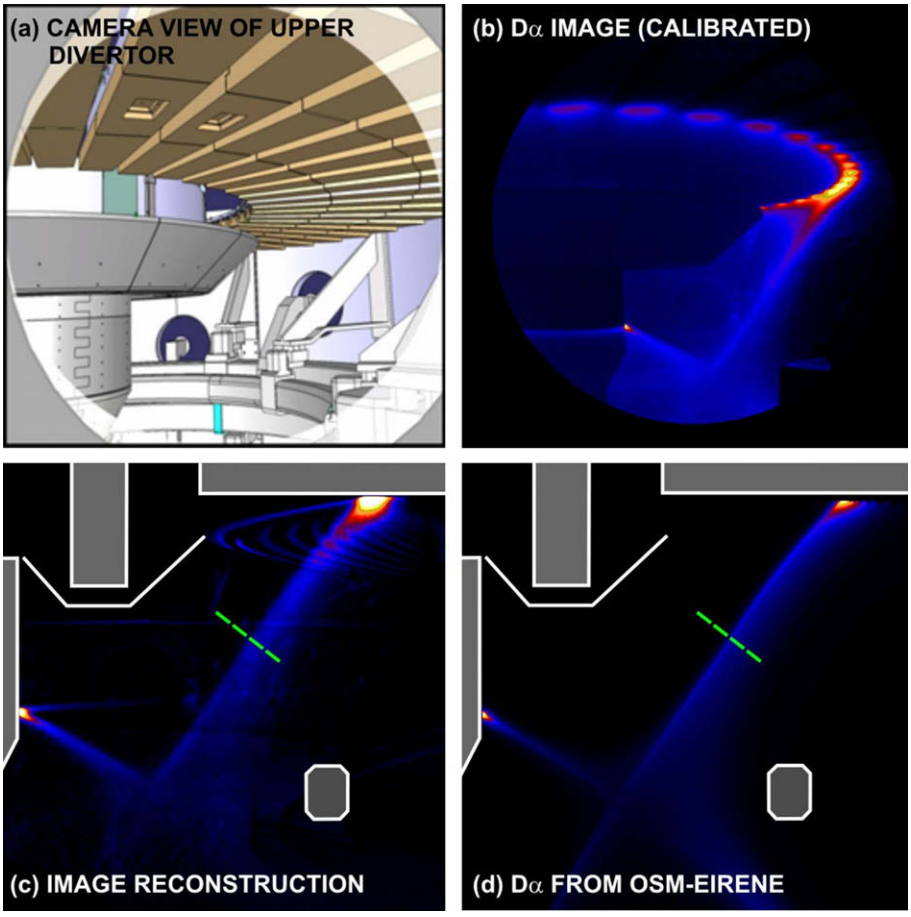

Fig. 1. Image analysis and comparison with OSM–EIRENE results. (a) Camera view of the upper divertor region in MAST, (b) calibrated D_α filtered image (18843@259 ms), (c) tomographically reconstructed D_α image, and (d) D_α profile calculated by OSM–EIRENE. The scales in (b) and (c) are the same, with a peak value of 4.0×10^{19} photons m^{-3} s^{-1}.

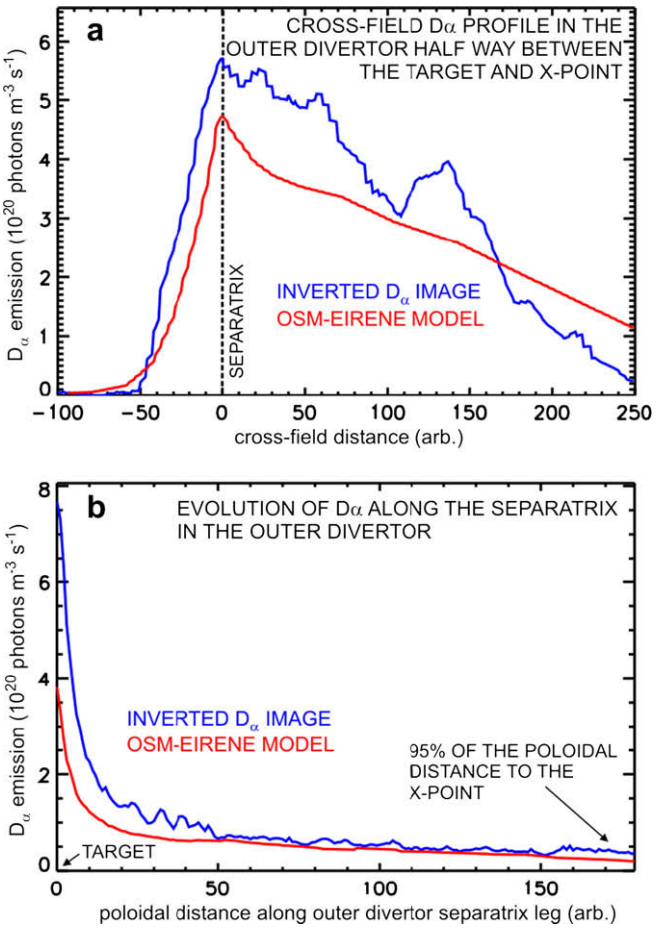

Fig. 2. Detailed comparison measured (blue) and OSM–EIRENE (red) calculated D_α profiles. (a) Cross-field D_α profile along the dashed line in Fig. 1(c) and (d). (b) Profiles along the outer divertor separatrix leg by generating a series of cross-field profiles as in (a) between the strike-point and the x-point, and taking the peak values. The target is at the origin of the horizontal axis. (For interpretation of the references to color in this figure legend, the reader is referred to the web version of this article).

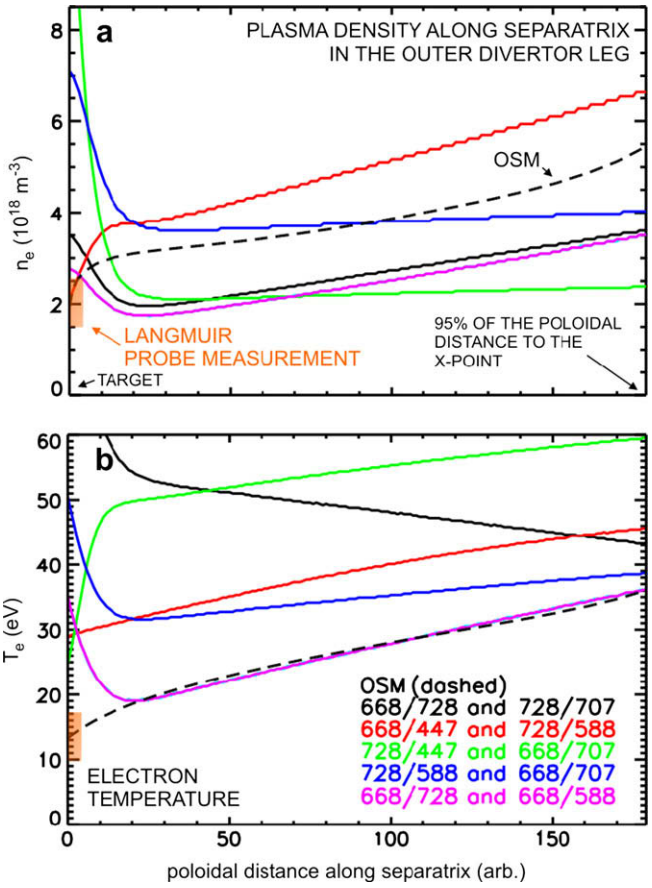

Fig. 3. Comparison of (a) n_e and (b) T_e profiles along the outer separatrix leg from helium line ratio analysis with results from OSM–EIRENE calculations. The key is found in (b), where the pairs of line ratios used to generate each profile are listed (see Section 4).

be on top of one another. The task now is to try and correlate the discrepancies with uncertainties in the atomic data, as in [11]; to assess contamination of the camera data by neighbouring lines, from comparison with multi-chord spectrometer data; and to refine the OSM transport model. Note that kinetic transport of helium excited states with EIRENE (not shown) indicates that meta-stables do not affect the above results.

Acknowledgements

Thanks to E. Hollmann for the idea. This work was funded jointly by the United Kingdom Engineering and Physical Sciences Research Council and by the European Communities under the contract of Association between EURATOM and UKAEA. The views and opinions expressed herein do not necessarily reflect those of the European Commission.

References

[1] E. de la Cal, Nucl. Instrum. and Meth. Phys. Res. A 403 (1998) 490.
[2] A.R. Field, P.G. Carolan, et al., Rev. Sci. Instrum. 70 (1) (1999) 355.
[3] Y. Andrews et al., J. Nucl. Mater. 266–269 (1999) 1234.
[4] R.F. Boivin, J.L. Kline, E.E. Scime, Phys. Plasma 8 (12) (2001) 5303.
[5] S. Kajita, N. Ohno, S. Takamura, T. Nakano, Phys. Plasma 13 (2006) 013301-1.
[6] S. Lisgo et al., J. Nucl. Mater. 337–339 (2005) 256.
[7] D. Reiter, The EIRENE Code, <http://www.eirene.de>.
[8] M. Anton, H. Weisen, et al., Plasma Phys. Control. Fus. 38 (1996) 1849.
[9] C.C. Paige, M.A. Saunders, ACM Trans. Math. Soft. 8 (1) (1982) 43.
[10] H.P. Summers et al., Plasma Phys. Control. Fus. 44 (2002) B323.
[11] Y. Andrews, M.G. O'Mullane, Plasma Phys. Control. Fus. 42 (2000) 301.